Induction of tracheal mesoderm and chondrocyte from pluripotent stem cells in mouse and human.

Keishi Kishimoto[1, 2, 3, 4], Kana T. Furukawa[1], Agustin LuzMadrigal[3, 4], Akira Yamaoka[1], Chisa Matsuoka[1], Masanobu Habu[5], Cantas Alev[5, 6], Aaron M. Zorn[2, 3, 4], and Mitsuru Morimoto[1, 2, *]

[1]Laboratory for Lung Development, Riken Center for Biosystems Dynamics Research (BDR), Kobe, 650-0047, Japan

[2]RIKEN BDR – CuSTOM Joint Laboratory, Cincinnati Children's Hospital Medical Center, Cincinnati, OH 45229, USA

[3]Center for Stem Cell & Organoid Medicine (CuSTOM), Cincinnati Children's Hospital Medical Center, Cincinnati, OH 45229, USA

[4]Division of Developmental Biology, Cincinnati Children's Hospital Medical Center, Cincinnati, OH 45229, USA

[5]Department of Cell Growth and Differentiation, Center for iPS Cell Research and Application (CiRA), Kyoto University, Kyoto 606-8507, Japan.

[6]Institute for the Advanced Study of Human Biology (ASHBi), Kyoto University, Kyoto 606-8501, Japan

*Corresponding author. Email: mitsuru.morimoto@riken.jp

Abstract (149 words)

The periodic cartilage and smooth muscle structures in mammalian trachea are derived from tracheal mesoderm, and tracheal malformation results in serious respiration defects in neonates. To establish a human tracheal mesodermal development model, an *in vitro* differentiation protocol from pluripotent stem cells was desired. Here we show that endodermal-to-mesodermal canonical Wnt signaling induces trachea progenitors in mouse splanchnic mesoderm. Loss of β-catenin in fetal mouse mesoderm caused loss of $Tbx4^+$ tracheal mesoderm and trachea cartilage agenesis. We found that endodermal Wnt ligands promote mesodermal Tbx4 expression independent of known Nkx2.1-mediated respiratory endoderm development. *In vitro*, activating Wnt and Bmp signaling in mouse ES cell (ESC)-derived lateral plate mesoderm (LPM) generated tracheal mesoderm containing chondrocytes and smooth muscle cells. For human ESC-derived LPM, SHH activation was required along with Wnt to generate authentic tracheal mesoderm. These findings are foundations for deriving human tracheal mesoderm for applications in tracheal tissue repair.

Main paragraph (2,036 words)

The mammalian respiratory system is crucial for postnatal survival, and defects in the development of the respiratory system cause life-threatening defects in breathing at birth[1]. The trachea is a large tubular air path that delivers external air to the lung. Abnormal development of the tracheal mesenchyme, including cartilage and smooth muscle (SM), is associated with congenital defects in cartilage and SM such as tracheoesophageal fistula (TEF) and tracheal agenesis (TA)[2, 3]. Thus, understanding tracheal development is crucial to better understand TEF/TA and establish a protocol to reconstruct trachea from pluripotent stem cells for human tissue repair.

Trachea/lung organogenesis is coordinated by endodermal-mesodermal interactions during embryogenesis. The primordial tracheal/lung endoderm appears at the ventral side of the anterior foregut at embryonic day 9 to 9.5 (E9.0–9.5) in mouse (Fig. 1a). Previous studies have revealed that development of tracheal/lung endoderm is initiated by graduated expression of mesodermal Wnt2/2b and Bmp4 expression along the dorsal-ventral axis[4-7]. This mesodermal-to-endodermal Wnt and Bmp signaling drives expression of Nkx2.1, the key transcription factor of tracheal/lung lineages[8], at the ventral side of the anterior foregut, which in turn suppresses Sox2 to segregate these $Nkx2.1^+$ endodermal cells from the esophageal lineage. The $Nkx2.1^+$ endoderm then invaginates into the ventral mesoderm to form the primordial trachea and lung buds. At the same time, the $Sox2^+$ endoderm at the dorsal side develops into the esophagus by E10.5 (Fig. 1a). By recapitulating developmental processes *in vitro*, tracheal/lung endodermal cells and differentiated epithelial populations have been generated from both mouse and human pluripotent stem cells[9-11], and can also be used for disease modeling[12-14]. However, an established protocol for inducing tracheal/lung mesoderm and differentiated mesenchymal tissue from pluripotent cells has not yet been reported because developmental signaling pathways coordinating the mesodermal development are still undefined.

The trachea mesoderm originates from splanchnic mesoderm, which is defined as the lateral plate

mesoderm (LPM) surrounding the endodermal organs. At the same time as endodermal Nkx2.1 induction, trachea/lung mesoderm is also defined, expressing Tbx4/5 by E10.5, which are markers for trachea/lung mesoderm and required for proper mesenchymal development (Fig. 1a)[15]. We previously reported that synchronized polarization of mesodermal cells and temporal initiation of cartilage development regulates tracheal tube morphogenesis by coordinating the length and diameter of the mouse trachea, respectively[16, 17]. However, the mechanism underlying the initial induction of trachea mesoderm is still unclear.

To study the initiation of the mesodermal development of the trachea, we validated the involvement of Nkx2.1 in mesodermal Tbx4 expression because endodermal-mesodermal interactions orchestrate organogenesis throughout development in general. Nkx2.1 is an endodermal transcription factor necessary for tracheal and lung development and its genetic ablation results in TEF[8]. We examined *Nkx2.1*^{null} mouse embryos and confirmed the TEF phenotype with a single tracheoesophageal (Tr-E) tube (Fig. 1b). Interestingly, *Nkx2.1*^{null} embryos retained Tbx4 expression in the ventrolateral mesoderm of a single Tr-E tube, although the segregation was defective (Fig. 1b), indicating that tracheal mesodermal induction is independent of endodermal Nkx2.1. We compared the phenotype of *Nkx2.1*^{null} with that of *Shh*^{Cre}, *Ctnnb1*$^{flox/flox}$ embryos which also show anterior foregut endoderm segregation defect and loss of Nkx2.1 expression (Fig. 1c and d)[4, 5]. In contrast to *Nkx2.1*^{null} embryos, *Shh*^{Cre}, *Ctnnb1*$^{flox/flox}$ embryos did not express Tbx4, suggesting the activation of endodermal Wnt signaling, but not Nkx2.1, is required for following mesodermal Tbx4 expression. Thus, the initial induction of trachea mesoderm is independent of known Nkx2.1-mediated respiratory endoderm development, but dependent on Wnt signaling at the ventral anterior foregut.

To further study the spatiotemporal regulation of canonical Wnt signaling during tracheoesophageal segregation at E9.5 to E11.5, we used a reporter line LEF1^{EGFP} and examined the distribution of EGFP in the canonical Wnt signaling response (Fig. 2a and b)[18]. At E9.5, EGFP was detected in the ventral

half of the anterior foregut endoderm where trachea endodermal cells appear and express Nkx2.1 (Fig. 2a and b, *arrowheads*). After E10.5, the EGFP reporter was activated in the surrounding mesoderm, and its intensity was increased at E11.5 (Fig. 2a and b, *arrowheads*). Because these $EGFP^+$ mesodermal cells expressed Tbx4 (Fig. 2b), we hypothesized that Wnt signaling in the early mesoderm is involved in the initiation of the tracheal mesoderm.

To validate the role of mesodermal Wnt signaling, we genetically ablated β-Catenin, a core component of canonical Wnt signaling, from embryonic mesoderm. We employed the Dermo1-Cre line which targets embryonic mesoderm, including trachea/lung mesoderm, and generated *Dermo1*^{Cre}, *Ctnnb1*$^{flox/flox}$ mice [19-22]. In the mutant embryos, Tbx4 expression was absent in the mesoderm at E10.5 (Fig. 2c), indicating that mesodermal canonical Wnt signaling is necessary for Tbx4 expression. In contrast, endodermal Nkx2.1 expression and tracheoesophageal segregation were not affected, indicating that mesodermal Wnt signaling and Tbx4 is dispensable for endodermal development. To our surprise, the mutant still developed lung buds and expressed Tbx4 in mesoderm (Supplementary Fig. S1a). Disruption of Wnt signaling in the mesoderm altered Tbx4 expression in the tracheal but not lung mesoderm, suggesting that Wnt-mediated mesodermal Tbx4 induction is a unique system in tracheal development but not lung development.

We further examined late developmental stages to determine whether cartilage and SM architectures are affected in *Dermo1*^{Cre}, *Ctnnb1*$^{flox/flox}$ embryos. In the mutants at E16.5, a periodic cartilage ring structure labeled with Sox9 failed to develop, and circumferential SM bundles labeled with smooth muscle actin (SMA), became randomized (Fig. 1d and d' and Supplementary Fig. S2. Therefore, mesodermal Wnt signaling is crucial for trachea mesenchymal development, and its defect results in the trachea cartilage agenesis phenotype.

Next, we sought to identify a source of Wnt ligands that initiates mesodermal Tbx4 expression. Due to essential role of Wnt2 at early trachea/lung development[4], we conducted *in situ* hybridization

for *Wnt2* and revealed transient expression of *Wnt2* in the ventrolateral mesoderm of the anterior foregut at E9.5, which was obviously reduced by E10.5 when Tbx4 was expressed (Figs. 2b and 3a). Wnt2 is most likely not involved in Tbx4 expression after E10.5. This observation prompted us to hypothesize that an endodermal-to-mesodermal interaction but not mesodermal autonomous induction is required for Tbx4 expression. To test this hypothesis, we generated Shh^{Cre}, $Wls^{flox/flox}$ mice, in which endodermal Wnt ligand secretion is inhibited by targeting *Wntless* (*Wls*) gene, which is essential for exocytosis of Wnt ligands[23]. This endoderm-specific deletion of *Wls* resulted in loss of Tbx4 expression in the mesoderm but retained Nkx2.1 expression in the endoderm and *Wnt2* in the mesoderm (Fig. 3b and c)[23], making these mice a phenocopy to $Dermo1^{Cre}$, $Ctnnb1^{flox/flox}$ mice (Fig. 2c). Shh^{Cre}, $Wls^{flox/flox}$ embryos also formed lung buds and expressed Tbx4 in the distal lung mesoderm (Supplementary Fig. S1b), supporting our idea that Wnt signaling in splanchnic mesoderm mainly contributes to initiation of mesodermal development of the trachea, but not of the lung.

These findings indicate that the endodermal Wnt ligands are sufficient for tracheal mesodermal development. From these observations, we conclude that mesodermal Wnt2 activates endodermal canonical Wnt signaling to express Nkx2.1 and Wnt ligands individually. These Wnt ligands then induce endodermal-to-mesodermal canonical Wnt signaling to initiate mesodermal Tbx4 expression (Fig. 3d). These results also suggest that specification in the trachea endodermal lineage is not necessary for the initial induction of the tracheal mesoderm.

To ask whether Wnt signaling is capable of initiating the differentiation of naïve mesodermal cells to $Tbx4^{+}$ tracheal mesodermal cells in *vitro*, we established a protocol for lateral plate mesoderm (LPM) induction from mouse ESCs by refining the published protocol for LPM induction from human pluripotent stem cells[24]. Because mouse and human ESCs show different states called naïve and primed, which correspond to pre- and post-implantation epiblasts, respectively, we converted mouse ESCs (mESCs) into an epiblast 'primed' state that led to middle-primitive streak (mid-PS) cells[25].

These mid-PS cells were then differentiated into LPM cells (Fig. 4a). At day 5, LPM induction was confirmed by immunocytochemistry for Foxf1 which is known as expressed in LPM including splanchnic mesoderm[26] (Fig. 4b). Given that previous mouse genetic studies have identified Bmp4 as a crucial regulator of tracheal development[6, 27], we tested whether canonical Wnt and Bmp4 signaling are sufficient to direct the differentiation of the LPM into the tracheal mesoderm ($Foxf1^+/Tbx4^+$). mESC-derived LPM cells were cultured with Wnt agonist (CHIR99021) and Bmp4 for 3 days and analysed by immunocytochemistry. The majority of cells were double positive for $Foxf1^+$ and $Tbx4^+$ at day 8, suggesting successful induction of the tracheal mesoderm (Fig. 4c). At day 12, importantly, $Sox9^+$ aggregated cell masses positive for Alcian blue staining appeared on the dish, indicative of chondrocytes (Fig. 4d, e). Smooth muscle cells (SMA^+ cells) concurrently appeared to show fibroblastic morphology and filled the spaces not filled by the $Sox9^+$ cells (Fig. 4d). These data suggest that the mESC-derived tracheal mesoderm is able to develop into tracheal mesenchyme, including chondrocytes and smooth muscle cells.

Finally, we tested the role of Wnt signaling in the human tracheal mesoderm using human ESCs (hESCs). Human LPM induction was performed by following an established protocol[24] (Fig. 4g). Subsequently, the cells were directed to tracheal mesoderm using a Wnt agonist and Bmp4. Because Tbx4 is also expressed in the limbs and other fetal mouse tissues[28], we sought additional genetic markers for the tracheal mesoderm. We searched the single-cell transcriptomics dataset of the developing splanchnic mesoderm at E9.5 and identified *Nkx6.1* as a marker for mesodermal cells surrounding the trachea, lung and oesophagus (Han et al., 2019, co-submitted to *Nature Cell Biol.*). The expression of *TBX4* and *NKX6.1* in the hESC-derived tracheal mesoderm was examined by qRT-PCR. Although *TBX4* was induced in a Wnt agonist dose-dependent manner, *NKX6.1* expression was not significantly elevated (Supplementary Fig. S3a), suggesting that human tracheal mesoderm development requires an additional factor to become more *in vivo*-like. Because the ventral LPM is

exposed to SHH in addition to Wnt and Bmp4 during tracheoesophageal segregation[29, 30], we assessed whether the SHH agonist (purmorphamine) can improve differentiation from hESC-derived LPM cells into the tracheal mesoderm (Fig. 4f and Supplementary Fig. S3b). As expected, both *TBX4* and *NKX6.1* expression was upregulated by the SHH agonist (Supplementary Fig. S3c). In this culture condition, the Wnt agonist enhanced the expression of the *TBX4* and *NKX6.1* genes in a dose-dependent manner (Fig. 4g, h). Further extended culture induced $SOX9^{+}$ chondrocytes in a Wnt activity-dependent manner (Fig. 4i, j). In this culture system, the removal of BMP4 from the growth factor cocktail did not affect differentiation, implying that exogenous BMP4 activation is dispensable (Fig. 4k-m). Because of the obvious upregulation of the endogenous *BMP4* gene in the hESC-derived LPM by day 2, endogenous BMP4 may be enough to induce tracheal mesoderm and chondrocytes (Fig. 4n). Taken together, these data suggest that Wnt signaling plays a unique role in driving differentiation into tracheal mesoderm and chondrocytes from the LPM, which is conserved between mice and humans.

This study demonstrated that endodermal-to-mesodermal canonical Wnt signaling is the cue that initiates tracheal mesodermal development in developing mouse embryos, which is independent of the previously known Nkx2.1-mediated respiratory tissue development. Based on our knowledge of developmental biology, we successfully generated tracheal mesoderm and chondrocytes from mouse and human ESCs. In our protocol, we stimulated ESC-derived LPM with Wnt, Bmp and SHH signaling to mimic spatial information of the ventral anterior foregut. For induction of respiratory endoderm, Wnt, Bmp and Fgf signaling are required to direct cells in anterior foregut to differentiate into the respiratory lineage[9-11]. Thus, Wnt and Bmp signaling are conserved factors that provide spatial information, while Fgf and SHH are required in endoderm and mesoderm induction, respectively, reflecting the unique signaling pathways in each tissue. Mesoderm induction may need fewer exogenous growth factors because the mesodermal cells themselves are a source of spatial information,

such as BMP4 in our protocol.

Recently, Han et al. delineated mesodermal development during organ bud specification using single-cell transcriptomics analyses of mouse embryos from E8.5 to E9.5 (Han et al., co-submitted to *Nature Cell Biol.*). Based on the trajectory of cell fates and signal activation, this group also generated organ-specific mesoderm, including respiratory mesoderm, from hESCs, thereby determining that Wnt, BMP4, SHH and retinoic acid direct differentiation of hESC-derived splanchnic mesoderm to respiratory mesoderm, supporting our current findings.

These culture methods could be a strong tool to study human organogenesis and the aetiology of TEA and TA, as well as to provide cellular resource for human tracheal tissue repair.

Methods

Mice

All mouse experiments were approved by the Institutional Animal Care and Use Committee of RIKEN Kobe Branch. Mice were handled in accordance with the ethics guidelines of the institute. *Nkx2.1*^{null}, *Shh*^{Cre}, *Dermo1*^{Cre}, *Ctnnb1*$^{flox/flox}$, *Wls*$^{flox/flox}$ mice were previously generated[16, 20, 31-33].

In all experiments, at least 3 embryos from more than 2 littermates were analyzed. All attempts for replicate were successful. Sample size was not estimated by statistical methods. No data was excluded in this study. All control and mutant embryos were analyzed. No blinding was done in this study.

Immunostaining

Mouse embryos were fixed by 4% Paraformaldehyde/PBS (PFA) overnight at 4°C. Specimens were dehydrated by ethanol gradient and embedded in paraffin. Paraffin sections (6-μm) were de-paraffinized and rehydrated for staining. Detailed procedure and antibodies of each staining were listed in Supplementary Table 1.

In situ hybridization

Mouse embryos were fixed with 4%PFA/PBS at 4°C overnight, and then tracheas were dissected. Specimens were incubated in sucrose gradient (10, 20, 30%) and embedded in OCT compound. Frozen sections (12-μm) were subjected to *in situ* hybridization. For probe construction, Wnt2 cDNA fragment amplified by following primers 5'- ATAGTCGACACAGAGATCACAGCCTCTTT -3' and 5'- ATAGAATTCCATGTCCTCAGAGTACAGGA -3'. This cDNA fragment was subcloned into pBluscript SK+ at *Eco*RI and *Sal*I sites. An antisense cRNA transcript for Wnt2 was synthesized with DIG labeling mix (Roche Life Science) and T3 RNA polymerase (New England Biolabs Inc.). Slides were permeabilized in 0.1% Triton-X100/PBS for 30min and blocked in acetylation buffer. After pre-

hybridization, slides were hybridized with 500ng/ml of DIG-labeled cRNA probes overnight at 65°C. After washing with SSC, slides were incubated with anti-DIG-AP antibodies (1:1000 Roche Life Science, 11093274910). Sections were colored with BM-purple (Roche Life Science, 11442074001).

Cell culture

EB3 (AES0139, RIKEN BioResorce Center) , a mouse ES cell line, was kindly provided by Dr. Hitoshi Niwa (Department of Pluripotent Stem Cell Biology, Institute of Molecular Embryology and Genetics in Kumamoto University)[34, 35]. Cells were maintained in 2i + leukemia inhibitory factor (LIF) media (1,000 units/ml LIF, 0.4μM PD0325901, 3μM CHIR99021 in N2B27 medium) on ornithine-laminin coated-dishes[25]. For mesodermal differentiation of mouse ES cells, cells were digested by TrypLE express (Thermo Fisher Scientific, 12604013) and seeded onto Matrigel-coated 12 well plate. EpiLC were induced by EpiLC differentiation medium (1% knockout serum, 20ng/ml Activin A, 12ng/ml FGF2, and 10μM Y27632 in N2B27 Medium)[25] for 2 days. Lateral plate mesoderm was established by Loh's protocol with some modification[24]. EpiLC cells were digested by TrypLE express to single cells and seeded onto Matrigel-coated 12 well plate at the density of $6x10^5$ cells/well. The cells around middle primitive streak was induced by LPM D2 medium composed of 2% B27 Supplement Serum free (Thermo Fisher Scientific, 17504044), 1 x GlutaMax (Thermo Fisher Scientific, 35050061), 20ng/ml basic FGF (Peprotech, AF-100-18B), 6μM CHIR99021 (Sigma Aldrich, SML1046), 40ng/ml BMP4 (R&D Systems, 5020-BP-010), 10ng/ml Activin A (Peprotech, PEP-120-14-10), 10μM Y27632 (Sigma Aldrich, Y0503) in Advanced DMEM (Thermo Fisher Scientific, 12491015) for 48 hours. After that, LPM was induced by LPM D4 medium composed of 2% B27 Supplement Serum free, 1 x GlutaMax, 2μM XAV939 (Sigma Aldrich, X3004), 2μM SB431542 (Merck, 616461), 30ng/ml human recombinant BMP4 in Advanced DMEM for 24 hours. At Day 5, respiratory mesenchyme was induced by Day5 medium composed of 2% B27 Supplement Serum free, 1 x GlutaMax, 1μM CHIR99021, 10ng/ml BMP4. Medium were freshly renewed every

day.

H1 (NIHhESC-10-0043 and NIHhESC-10-0062), human embryonic stem cell, was provided by cincinnati children's hospital medical center Pluripotent Stem Cell Facility. Cells were maintained in mTeSR1 medium (Stem Cell Technologies) on Matrigel-coated plate. For differentiation of H1 cells to mesodermal cells, confluent cells were digested by Accutase to single cells and seeded onto Geltrex-coated 12well plate at the dilution of 1:20 – 1:18 in mTeSR1 with 1uM Thiazovivin (Tocris). Next day, the cells around middle primitive streak were induced by cocktails of 6μM CHIR99021 (Sigma Aldrich, SML1046), 40ng/ml BMP4 (R&D Systems, 5020-BP-010), 30ng/ml Activin A (Cell Guidance Systems), 20ng/ml basic FGF (Thermo Fisher Scientific) and 100nM PIK90 (EMD Millipore) in Advanced DMEM/F12 including 2% B27 Supplement minus vitamin A, 1% N2 Supplement, 10uM Hepes, 100UI/mL Penicillin/Streptomycin, 2mM L-glutamine for 24 hours. After that, LPM was induced by LPM D2 medium composed of 1μM Wnt C59 (Cellagen Technologies), 1μM A83-01 (Tocris), 30ng/ml human recombinant BMP4 in Advanced DMEM/F12 including 2% B27 Supplement minus V. A., 1 x N2 Supplement, 10uM Hepes, 100UI/mL Penicillin/Streptomycin, 2mM L-glutamine for 24 hours. To generate respiratory mesenchyme, we combined 3uM CHIR99021, 2uM Purmorphamine (Tocris), and 10ng/ml Bmp4 in Advanced DMEM/F12 medium including 2% B27 Supplement Serum free, 1 x N2 Supplement, 10uM Hepes, 100UI/mL Penicillin/Streptomycin, 2mM L-glutamine from Day 2 to Day10. Medium was freshly renewed everyday

Immunocytochemistry

At differentiating process, cells were fixed by 4% PFA for 10 minutes at room temperature. For intracellular staining, cells were permeabilized by 0.2% TritonX-100/PBS for 10 minutes at room temperature. After blocking the cells with 5% normal donkey serum, cells were incubated with primary antibodies overnight at 4°C. Then, cells were incubated with secondary antibodies for 1hr at

room temperature. Detailed procedure and antibodies of each staining were listed in Supplementary Table 2.

Alcian blue staining

Cells were fixed in 4% PFA/PBS for 10minute at room temperature. After washing with PBS, cells were incubated with 3% acetic acid for 3 minutes and then stained with 1% alcian blue/3% acetic acid for 20 minutes.

Quantitative RT-PCR

Total mRNA was isolated by using the Nucleospin kit (TaKaRa, 740955) according to manufacturer's procedure. cDNA was synthesized by Super™Script™ VILO cDNA synthesis kit (Thermo Fisher Scientific, 11754050). qPCR was performed by PowerUp™ SYBR™ Green Master Mix on QuantStudio 3 or 6. Primer sequences were listed on Supplementary Table 3. Data are expressed as a Fold Change and were normalized with undifferentiated cells expression.

Statistical analyses

Statistical analyses were performed with Excel2013 (Microsoft) or PRISM8 (GraphPad software). For multiple comparison, one-way ANOVA and Tukey's methods were applied. For paired comparison, statistic significance was determined by F-test and Student's or Welch's two-tailed t test.

Acknowledgements

We thank Hinako M Takase and Hiroshi Hamada for Wntless conditional flox mice, Hiroshi Niwa for EB3, mouse ES cells, and Animal Resource Development Unit. We also thank Yuka Noda and David Luedeke for general technical support. We also thank Shigeo Hayashi for primary reading.

These studies are supported by the funding from Grants-in-Aid for Scientific Research (B)(17H04185)(M.M.), Young Scientists (17K15133 and 19K16156)(K.K.) of the Ministry of Education, Culture, Sports, Science and Technology, Japan, and from The Takeda Science Foundation for the Life Science (M.M.), and The Uehara Memorial Foundation (K.K.). Partially supported by grant NICHD P01HD093363 to AMZ.

Author contributions

K.K., and M.M. designed the project and performed experiments with the aid of A.L.M., A.Y., C. M., and K.T.F.. Z.A. analyzed single cell transcriptomics for definitive endoderm and splanchnic mesoderm. A.L.M. supported human ES cell experiments, A.Y. supported mouse experiments. K.T. F. and C.M. performed mouse ES cell experiment. C. A. and M.H. contributed to mouse and human embryonic-stem cell-based lateral plate mesoderm induction and differentiation experiments.

K.K. and M.M. wrote the manuscript with the contribution of all authors.

Competing interests

The authors declare no competing interests.

Data availability

The authors declare that all data supporting the findings of this study are available within the article and its Supplementary Information files or from the corresponding author upon reasonable request. The datasets generated during the current studies are available in the System Science of Biological Dynamics (SSBD) database (http://ssbd.qbic.riken.jp/).

References

1. Morrisey, E.E. & Hogan, B.L. Preparing for the first breath: genetic and cellular mechanisms in lung development. *Dev Cell* **18**, 8-23 (2010).
2. Carden, K.A., Boiselle, P.M., Waltz, D.A. & Ernst, A. Tracheomalacia and tracheobronchomalacia in children and adults: an in-depth review. *Chest* **127**, 984-1005 (2005).
3. Landing, B.H. & Dixon, L.G. Congenital malformations and genetic disorders of the respiratory tract (larynx, trachea, bronchi, and lungs). *Am Rev Respir Dis* **120**, 151-185 (1979).
4. Goss, A.M. *et al.* Wnt2/2b and beta-catenin signaling are necessary and sufficient to specify lung progenitors in the foregut. *Dev Cell* **17**, 290-298 (2009).
5. Harris-Johnson, K.S., Domyan, E.T., Vezina, C.M. & Sun, X. beta-Catenin promotes respiratory progenitor identity in mouse foregut. *Proc Natl Acad Sci U S A* **106**, 16287-16292 (2009).
6. Domyan, E.T. *et al.* Signaling through BMP receptors promotes respiratory identity in the foregut via repression of Sox2. *Development* **138**, 971-981 (2011).
7. Kadzik, R.S. & Morrisey, E.E. Directing lung endoderm differentiation in pluripotent stem cells. *Cell Stem Cell* **10**, 355-361 (2012).
8. Minoo, P., Su, G., Drum, H., Bringas, P. & Kimura, S. Defects in tracheoesophageal and lung morphogenesis in Nkx2.1(-/-) mouse embryos. *Dev Biol* **209**, 60-71 (1999).
9. Gotoh, S. *et al.* Generation of alveolar epithelial spheroids via isolated progenitor cells from human pluripotent stem cells. *Stem Cell Reports* **3**, 394-403 (2014).
10. Longmire, T.A. *et al.* Efficient derivation of purified lung and thyroid progenitors from embryonic stem cells. *Cell Stem Cell* **10**, 398-411 (2012).
11. Mou, H. *et al.* Generation of multipotent lung and airway progenitors from mouse ESCs and patient-specific cystic fibrosis iPSCs. *Cell Stem Cell* **10**, 385-397 (2012).
12. Korogi, Y. *et al.* In Vitro Disease Modeling of Hermansky-Pudlak Syndrome Type 2 Using Human Induced Pluripotent Stem Cell-Derived Alveolar Organoids. *Stem Cell Reports* **12**, 431-440 (2019).
13. Jacob, A. *et al.* Differentiation of Human Pluripotent Stem Cells into Functional Lung Alveolar Epithelial Cells. *Cell Stem Cell* **21**, 472-488.e410 (2017).
14. Chen, Y.W. *et al.* A three-dimensional model of human lung development and disease from pluripotent stem cells. *Nat Cell Biol* **19**, 542-549 (2017).
15. Arora, R., Metzger, R.J. & Papaioannou, V.E. Multiple roles and interactions of Tbx4

and Tbx5 in development of the respiratory system. *PLoS Genet* **8**, e1002866 (2012).

16. Kishimoto, K. *et al.* Synchronized mesenchymal cell polarization and differentiation shape the formation of the murine trachea and esophagus. *Nat Commun* **9**, 2816 (2018).
17. Yin, W. *et al.* The potassium channel KCNJ13 is essential for smooth muscle cytoskeletal organization during mouse tracheal tubulogenesis. *Nat Commun* **9**, 2815 (2018).
18. Currier, N. *et al.* Dynamic expression of a LEF-EGFP Wnt reporter in mouse development and cancer. *Genesis* **48**, 183-194 (2010).
19. Yu, K. *et al.* Conditional inactivation of FGF receptor 2 reveals an essential role for FGF signaling in the regulation of osteoblast function and bone growth. *Development* **130**, 3063-3074 (2003).
20. Brault, V. *et al.* Inactivation of the beta-catenin gene by Wnt1-Cre-mediated deletion results in dramatic brain malformation and failure of craniofacial development. *Development* **128**, 1253-1264 (2001).
21. Hou, Z. *et al.* Wnt/Fgf crosstalk is required for the specification of basal cells in the mouse trachea. *Development* **146** (2019).
22. De Langhe, S.P. *et al.* Formation and differentiation of multiple mesenchymal lineages during lung development is regulated by beta-catenin signaling. *PLoS One* **3**, e1516 (2008).
23. Snowball, J., Ambalavanan, M., Whitsett, J. & Sinner, D. Endodermal Wnt signaling is required for tracheal cartilage formation. *Dev Biol* **405**, 56-70 (2015).
24. Loh, K.M. *et al.* Mapping the Pairwise Choices Leading from Pluripotency to Human Bone, Heart, and Other Mesoderm Cell Types. *Cell* **166**, 451-467 (2016).
25. Hayashi, K. & Saitou, M. Generation of eggs from mouse embryonic stem cells and induced pluripotent stem cells. *Nat Protoc* **8**, 1513-1524 (2013).
26. Kalinichenko, V.V., Gusarova, G.A., Shin, B. & Costa, R.H. The forkhead box F1 transcription factor is expressed in brain and head mesenchyme during mouse embryonic development. *Gene Expr Patterns* **3**, 153-158 (2003).
27. Li, Y., Gordon, J., Manley, N.R., Litingtung, Y. & Chiang, C. Bmp4 is required for tracheal formation: a novel mouse model for tracheal agenesis. *Dev Biol* **322**, 145-155 (2008).
28. Menke, D.B., Guenther, C. & Kingsley, D.M. Dual hindlimb control elements in the Tbx4 gene and region-specific control of bone size in vertebrate limbs. *Development* **135**, 2543-2553 (2008).
29. Han, L. *et al.* Osr1 functions downstream of Hedgehog pathway to regulate foregut

development. *Dev Biol* **427**, 72-83 (2017).

30. Rankin, S.A. *et al.* A Retinoic Acid-Hedgehog Cascade Coordinates Mesoderm-Inducing Signals and Endoderm Competence during Lung Specification. *Cell Rep* **16**, 66-78 (2016).
31. Harfe, B.D. *et al.* Evidence for an expansion-based temporal Shh gradient in specifying vertebrate digit identities. *Cell* **118**, 517-528 (2004).
32. Sosic, D., Richardson, J.A., Yu, K., Ornitz, D.M. & Olson, E.N. Twist regulates cytokine gene expression through a negative feedback loop that represses NF-kappaB activity. *Cell* **112**, 169-180 (2003).
33. Carpenter, A.C., Rao, S., Wells, J.M., Campbell, K. & Lang, R.A. Generation of mice with a conditional null allele for Wntless. *Genesis* **48**, 554-558 (2010).
34. Niwa, H., Masui, S., Chambers, I., Smith, A.G. & Miyazaki, J. Phenotypic complementation establishes requirements for specific POU domain and generic transactivation function of Oct-3/4 in embryonic stem cells. *Mol Cell Biol* **22**, 1526-1536 (2002).
35. Ogawa, K., Matsui, H., Ohtsuka, S. & Niwa, H. A novel mechanism for regulating clonal propagation of mouse ES cells. *Genes Cells* **9**, 471-477 (2004).

Figure 1

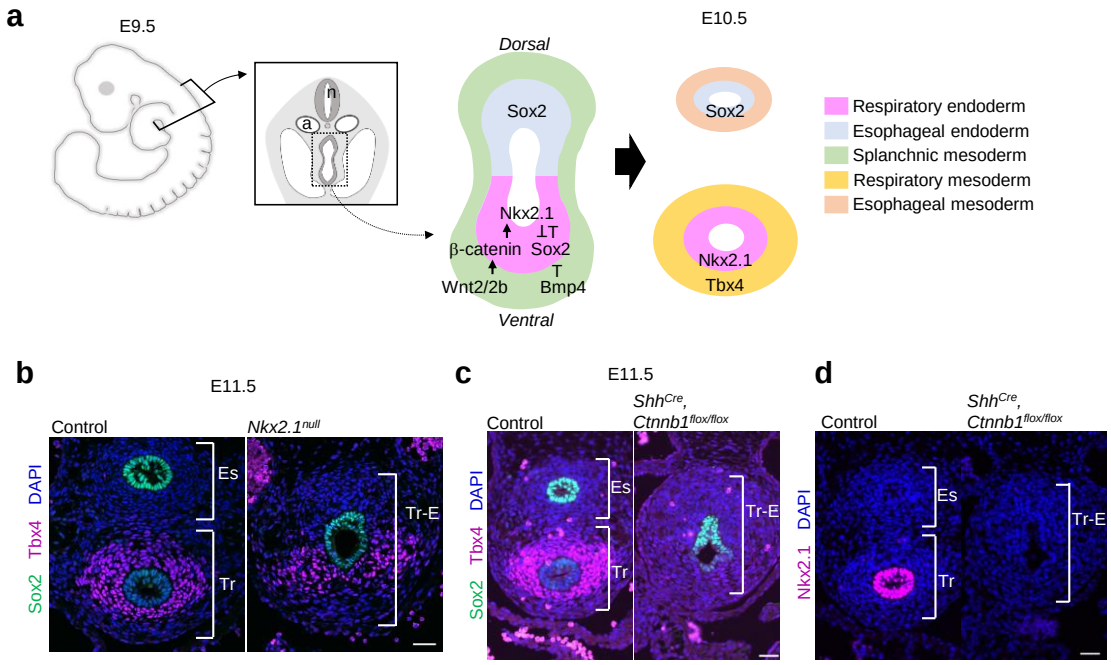

Figure 1 Activation of Wnt signalling in endoderm, but not Nkx2.1 expression, is activated to promote mesodermal development of the mouse trachea.

a, Schematic model of tracheoesophageal segregation.

b, Transverse sections of *Nkx2.1*^{null} mouse embryos and littermate controls. Sections were stained for Sox2 (*green*), Tbx4 (*magenta*), and DAPI (*blue*).

c, Transverse sections of *Shh*^{Cre}, *Ctnnb1*$^{flox/flox}$ mouse embryos and littermate controls. Sections were stained by Sox2 (*green*), Tbx4 (*magenta*), and DAPI (*blue*).

d, Transverse sections of *Shh*^{Cre}, *Ctnnb1*$^{flox/flox}$ mouse embryos and littermate controls. Sections were stained by Nkx2.1 (*magenta*) and DAPI (*blue*).

Scale bar, 40μm

Figure 2

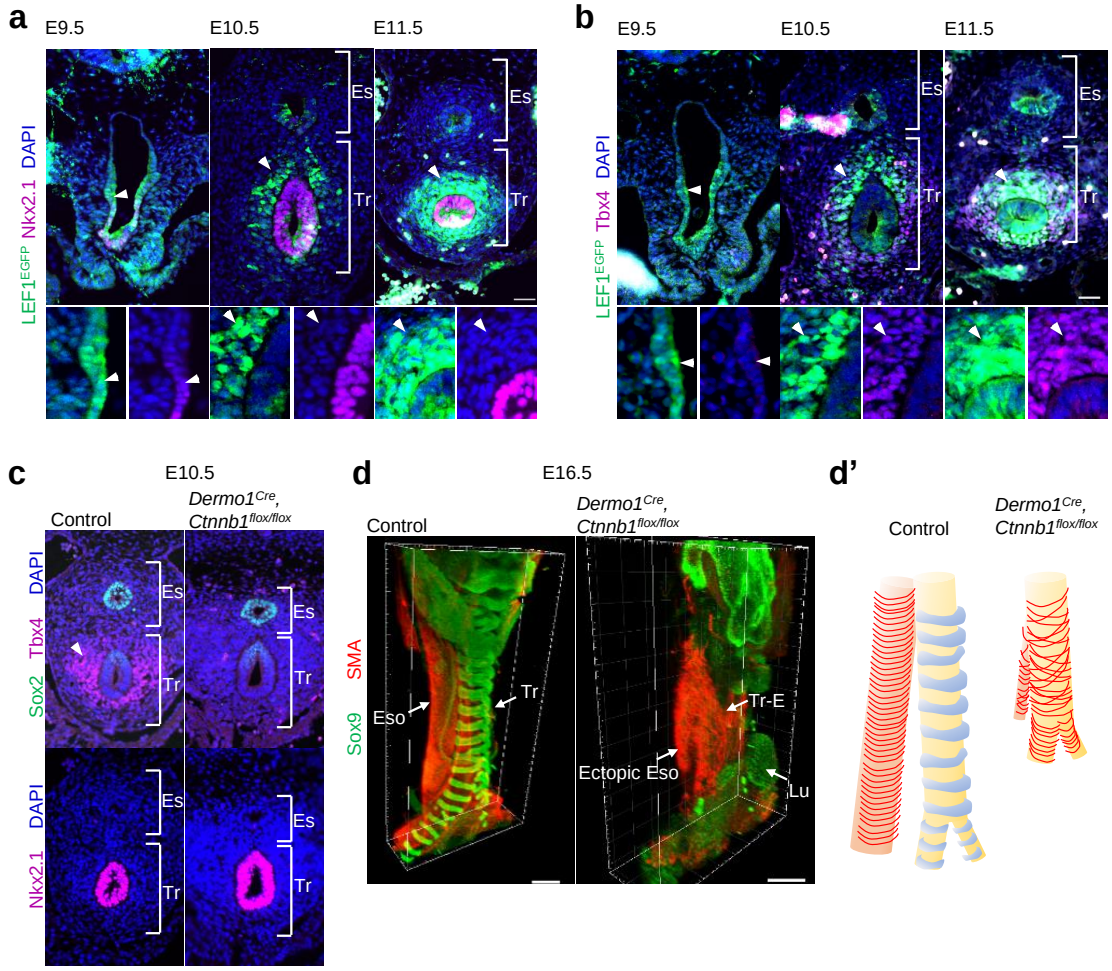

Figure 2 Wnt signalling is activated to promote mesodermal development of the mouse trachea.

a, Transverse sections of LEF1^{EGFP} reporter mouse embryos at E9.5 to E11.5. Sections were stained for EGFP (*green*), Nkx2.1 (*magenta*), and DAPI (*blue*). Arrowheads indicate GFP^{+} cells.

b, Transverse sections of LEF1^{EGFP} reporter mouse embryos at E9.5 to E11.5. Sections were stained for EGFP (*green*), Tbx4 (*magenta*), and DAPI (*blue*). Arrowheads indicate GFP^{+} cells.

c, Transverse sections of *Dermo1^{Cre}, Ctnnb1$^{flox/flox}$* mouse embryos and littermate controls at E10.5. Upper panels show sections stained for Sox2 (*green*), Tbx4 (*magenta*), and DAPI (*blue*). Lower panels show sections stained for Nkx2.1 (*magenta*) and DAPI (*blue*).

d, Three-dimensional imaging of whole trachea and oesophagus tissue at E16.5. Cartilage morphology and smooth muscle architecture in the tracheas of *Dermo1^{Cre}, Ctnnb1$^{flox/flox}$* mouse embryos and control littermates. Whole trachea and oesophagus were stained for Sox9 (*green*) and SMA (*red*).

d', Model of tracheal architecture in *Dermo1^{Cre}, Ctnnb1$^{flox/flox}$* mouse embryos and control littermates based on (**d**). Eso; Oesophagus, Lu; Lung, Tr; Trachea, Tr-E; Tracheoesophageal tube**.**

Scale bar: 40 μm (a, b, c), 300 μm (d).

Figure 3

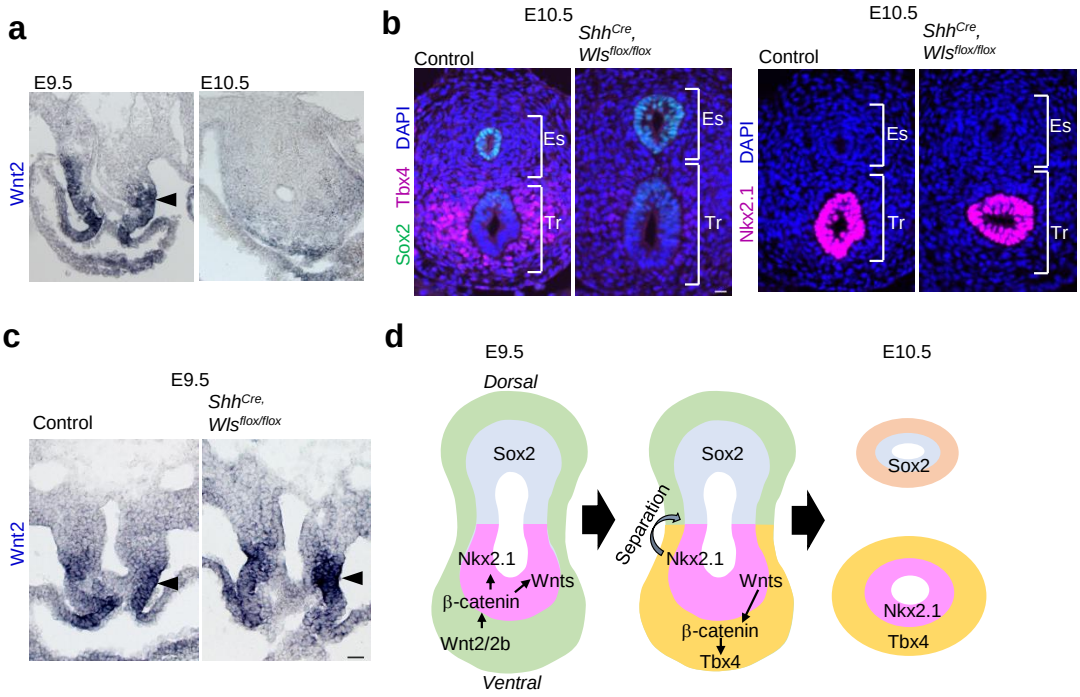

Figure 3 Endodermal Wnt ligands induce Tbx4 expression for tracheal mesoderm development of mouse trachea.

a, *In situ* hybridization for *Wnt2* mRNA during tracheoesophageal segregation. An arrowhead indicates *Wnt2* expression in the ventrolateral mesoderm at E9.5 and E10.5.

b, Transverse sections of Shh^{Cre}, $Wls^{flox/flox}$ mouse embryos and littermate controls at E10.5. Left panels show sections stained with Sox2 (*green*), Tbx4 (*magenta*), and DAPI (*blue*). Right panels show sections stained for Nkx2.1 (*magenta*) and DAPI (*blue*).

c, *In situ* hybridization for Wnt2 mRNA in Shh^{Cre}, $Wls^{flox/flox}$ mouse embryos and littermate controls at E9.5. Arrowheads indicate Wnt2 expression in the ventrolateral mesoderm.

d, Refined model of tracheoesophageal segregation and tracheal mesodermal differentiation

Eso; Oesophagus, Lu; Lung, Tr; Trachea.

Scale bar; 40 μm.

Figure 4

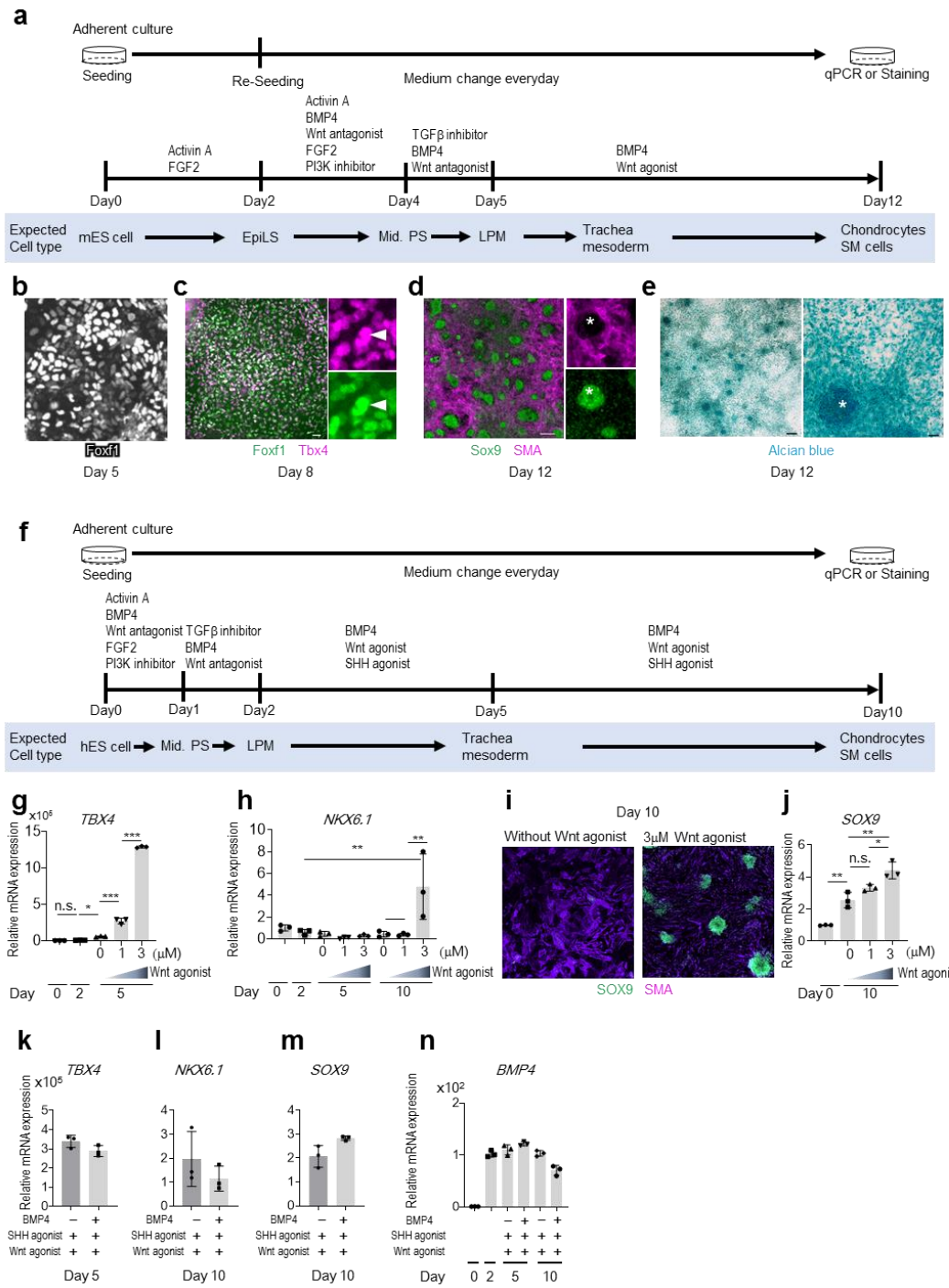

Figure 4 Generation of tracheal mesodermal cells and chondrocytes from mouse and human ESCs *in vitro.*

a, Experimental design to generate tracheal mesoderm from mESCs.

b, Differentiating cells from mESCs at day 5. Cells were stained for Foxf1 (*grey*).

c, Differentiating cells from mESCs at day 8. Cells were stained for Foxf1 (*green*) and Tbx4 (*magenta*). Arrowheads indicate $Tbx4^{+}$/$Foxf1^{+}$ mesodermal cells.

d, Differentiating cells from mESCs at day 12. Cells were stained for SMA (*magenta*) and Sox9 (*green*). The asterisk indicates $Sox9^{+}$/SMA^{-} chondrocyte aggregates.

e, Differentiating cells from mESCs at day 12. Chondrocytes were stained with Alcian blue. The asterisk indicates one of the chondrocyte aggregates.

f, Experimental design to generate tracheal mesoderm from hESCs

g, h, Results of qRT-PCR for *TBX4* (**g**) and *NKX6.1* (**h**) expression in differentiating hESCs. hESCs were incubated with growth factor cocktails including SHH agonist, BMP4 and different doses of Wnt agonist.

i, hESC-derived tracheal mesodermal cells cultured with/without Wnt agonist at day 10. Cells were stained for SMA (*magenta*) and SOX9 (*green*).

j, Results of qRT-PCR for *SOX9* expression of hESC-derived tracheal mesodermal cells at day 10 with different doses of Wnt agonist.

k-m, Results of qRT-PCR of *TBX4* (**k**), *NKX6.1* (**l**), *SOX9* (**m**) in differentiating hESCs cultured with/without BMP4.

n, Results of qRT-PCR for *BMP4* expression in differentiating hESCs at different time points. hESCs were cultured with/without BMP4.

Each column show the mean with S.D. *p<0.05, **p<0.005, ***p<0.0001